

# Experimental observation of a photonic hook

Cite as: Appl. Phys. Lett. **114**, 031105 (2019); doi: [10.1063/1.5065899](https://doi.org/10.1063/1.5065899)

Submitted: 11 October 2018 · Accepted: 07 January 2019

I. V. Minin,<sup>1,a)</sup> O. V. Minin,<sup>1,2</sup> G. M. Katyba,<sup>3,4</sup> N. V. Chernomyrdin,<sup>4,5,6</sup> V. N. Kurlov,<sup>3,5</sup> K. I. Zaytsev,<sup>4,5,6,b)</sup>  
L. Yue,<sup>7</sup> Z. Wang,<sup>7</sup> and D. N. Christodoulides<sup>8</sup>

## AFFILIATIONS

<sup>1</sup> Tomsk Politechnical University, Tomsk 634050, Russia

<sup>2</sup> Tomsk State University, Tomsk 634050, Russia

<sup>3</sup> Institute of Solid State Physics of the Russian Academy of Sciences, Chernogolovka 142432, Russia

<sup>4</sup> Bauman Moscow State Technical University, Moscow 105005, Russia

<sup>5</sup> Institute of Regenerative Medicine, Sechenov First Moscow State Medical University, Moscow 119991, Russia

<sup>6</sup> Prokhorov General Physics Institute of the Russian Academy of Sciences, Moscow 119991, Russia

<sup>7</sup> School of Electronic Engineering, Bangor University, Bangor LL57 1UT, United Kingdom

<sup>8</sup> College of Optics/CREOL, University of Central Florida, Orlando, Florida 32816, USA

<sup>a)</sup> Electronic mail: [prof.minin@gmail.com](mailto:prof.minin@gmail.com)

<sup>b)</sup> Electronic mail: [kirzay@gmail.com](mailto:kirzay@gmail.com)

## ABSTRACT

In this letter, we reported the experimental observation of a photonic hook (PH)—a type of near-field curved light generated at the output of a dielectric cuboid, featuring a broken symmetry and dimensions comparable to the electromagnetic (EM) wavelength. Given that the specific value of the wavelength is not critical once the mesoscale conditions for the particle are met, we verified these predictions experimentally using a 0.25 THz continuous-wave source. The radius of curvature associated with the PH-generated is smaller than the wavelength, while its minimum beam-waist is about  $0.44\lambda$ . This represents the smallest radius of curvature ever recorded for any EM beam. The observed phenomenon is of potential interest in optics and photonics, particularly, in super-resolution microscopy, manipulation of particles and liquids, photolithography, and material processing. Finally, it has a universal character and should be inherent to acoustic and surface waves, electrons, neutrons, protons, and other beams interacting with asymmetric mesoscale obstacles.

The idea that light propagates along straight lines is known since antiquity. The development of Maxwell's electrodynamics further reinforced these notions by ensuring the conservation of electromagnetic (EM) momentum. The possibility that a wavepacket can freely accelerate even in the absence of an external force was first discussed four decades ago<sup>1</sup> within the context of quantum mechanics. Namely, this is only possible as long as the quantum wavefunction follows an Airy-function profile. In 2007, this Airy self-acceleration process was first suggested and then observed experimentally.<sup>2,3</sup> Ever since, this class of accelerating or self-bending beams has attracted considerable attention and found applications in many diverse fields. In the past few years, other types of Airy-like accelerating curved beams have been intensely explored; among them are the “half-Bessel,”<sup>4</sup> Weber,<sup>5</sup> and Mathieu<sup>6</sup> beams, to mention a few. In all cases, these Airy-like wavefronts propagate on a

ballistic trajectory over a considerable distance. They still remain the only example of a “curved light transport” in nature.

On the other hand, the interaction of light with transparent spherical particles has been heavily investigated over the years since the days of Pliny the Elder (AD 23–AD 79).<sup>7</sup> By following the Mie formalism,<sup>8</sup> one could easily analyze a transformation of the EM field structure from that produced by a small dipole (in the Rayleigh limit<sup>9</sup>) to a pronounced jet-like caustic formed near the outer part of a particle, as a function of its geometry, dimensions, and optical properties.<sup>10,11</sup> In 2004, Chen *et al.* coined a new term “photonic nanojet” (PJ) for the sub-wavelength-scale focusing at the shadow side of a mesoscale dielectric particle.<sup>11</sup> By increasing the dimensions of a particle, the EM field structure evolves and tends to be more localized and directed forward.<sup>12</sup> Despite the beneficial performance of PJs in a number of applications, up to date, they have been generated primarily by

symmetric dielectric particles, while no attention has been paid to asymmetric mesoscale obstacles and to the formation of curved PJs.

In 2015, a new type of subwavelength curved PJ was proposed—a photonic hook (PH).<sup>13</sup> This prospect was identified by means of numerical analysis of EM field localization behind a dielectric three-dimensional (3D) particle with a broken symmetry.<sup>13,14</sup> But at present, no direct experimental confirmation of this phenomenon has been reported yet. This might be due to both difficulties in fabrication of micro-scale particles with high precision and the limited resolution of existing 3D sub-wavelength-resolution imaging modalities in the visible range. Moreover, in a realistic optical band system, for handling the asymmetric dielectric particle, it would need to be in contact with a finite-size dielectric substrate, which generates its own scattered field, interacting with that of a particle, thus leading to image distortions. Thereby, it could be a challenge today for experimental demonstration of the PH phenomenon in the optical domain. However, taking into account that the specific value of the incident wavelength is not critical (as long as the meso-scale conditions of a particle are satisfied),<sup>13</sup> detailed emulation experiments with terahertz (THz) radiation pave the way for advanced investigation and design and proof of concept demonstrations.

In this letter, we verify experimentally the existence of Minins' PH phenomenon. We demonstrate the PH effect using a continuous-wave scanning-probe microscope, operating at 0.25 THz. The observed experimental results agree with our theoretical predictions.

For our demonstration, as a representative PH source, we use an asymmetric dielectric particle (ADP) with a simple geometry, which implies appending a triangular prism to the front side of a cuboid,<sup>14</sup> see Fig. 1. We select polymethylpentene (TPX), the refractive index is  $n = 1.46$  at 0.25 THz<sup>15</sup> as a material platform for fabrication of this particle. Prior to fabrication of the particle, we perform numerical analysis of the PH formation, optimizing a cuboid rib length  $L$  and an angle of the appended prism  $\theta$ , as well as studying an impact of the AOP refractive index  $n$  on the PH geometry. In Fig. 2, we illustrate PH evaluation with changes of  $\theta$  and  $n$ . For this aim, we used the finite integral technique realized in commercial software—the CST Microwave Studio.

The phenomenon of focus bending the dielectric particle is caused by the interference of waves inside it as the phase velocity disperses. Due to the shape of the particle with broken

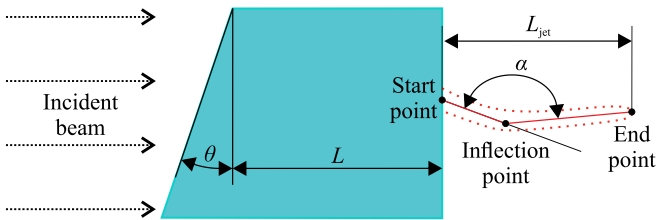


FIG. 1. Scheme of the PH formation behind ADP.

symmetry, the time of the complete phase of the wave oscillations varies irregularly in the particle.<sup>14</sup> As a result, the emitted light beam bends. It is worth noting that the PH is formed in the spatial region where the effects of near-field scattering (evanescent fields) play a significant role. As defined in Ref. 14, the PH curvature is determined by a midline  $L_{\text{jet}}$  aided by an angle  $\alpha$  between the two lines, which link the start point with the inflection point and the inflection point with the end point, respectively, see Fig. 1. We found that the TPX cuboid featuring the rib length of  $L = 4.8$  mm and the prism angle of  $\theta = 18.4^\circ$  ensures generation of PH with the maximal curvature, as shown in Fig. 2(e).

The shape and curvature radius of PH can be adjusted by varying wavelengths, incident light polarization, and geometric and optical parameters of the emitting particle.<sup>14</sup> The PH entirely matches the trend of power flows in a certain shadow region. In particular, it follows from a comparison of Figs. 2(b), 2(e), and 2(h) that with an increase in the refractive index from 1.40 to 1.52, the curvature of the PH changes its orientation on the opposite. We should also stress that, for the particular type of asymmetric dielectric particle, we could observe generation of a pronounced PH only in case if it is illuminated from the side of a prism,<sup>14</sup> while for all other orientations, the PH strongly distorts or even disappears.

In order to experimentally showcase the PH phenomenon, we fabricated the developed dielectric particle with an optimal geometry from a bulk piece of TPX by its mechanical shaping using a milling machine. To probe the 3D structure of the EM field behind this particle, we assembled an experimental setup relying on the principles of fiber-based scanning-probe THz imaging,<sup>16</sup> see Fig. 3. As a source of continuous-wave THz radiation, we use a backward-wave oscillator (BWO)<sup>17</sup> equipped with a wire-grid linear polarizer. In order to visualize the spatial distribution of EM field intensity  $|E|^2$  behind the cuboid, we applied a 2D-scanning system, which is similar to that described in Ref. 18 and an optical probe made of a flexible 300- $\mu\text{m}$ -diameter sapphire fiber with flat ends.<sup>19</sup> Thanks to rather low THz-wave absorption in sapphire,<sup>20</sup> this fiber allows for guiding the THz waves over tens of centimeters. Furthermore, a high refractive index of sapphire<sup>19</sup> leads to strong confinement of guiding modes in a fiber and, thus, yields sub-wavelength resolution imaging. The lateral spatial resolution of the described imaging approach is limited by the fiber diameter—i.e., 300- $\mu\text{m}$ -resolution (or  $\lambda/4$ ) for the employed fiber. The depth resolution is limited by the step and accuracy of the raster-scan; thus, we could expect it to be 100  $\mu\text{m}$ .

Finally, in Fig. 4, we present the results of PH visualization. From Fig. 4, we notice that the PH curvature is about  $\alpha = 148^\circ$ , while its length is  $L_{\text{jet}} < 2\lambda$  with the inflection point spaced by  $Z = 1.2\lambda$  from the back flat surface of ADP. It is important to note that the PH curvature radius is smaller than the wavelength. In turn, the Airy beam's characteristic diameter is related to the lens numerical aperture, usually amounting to tens of wavelengths, with the Airy beam's path length being related to the optical element diameter.<sup>2,3</sup> From the table-inset in Fig. 4, we observe that the lateral dimensions of PH are also sub-wavelength; thus, the PH phenomenon could provide

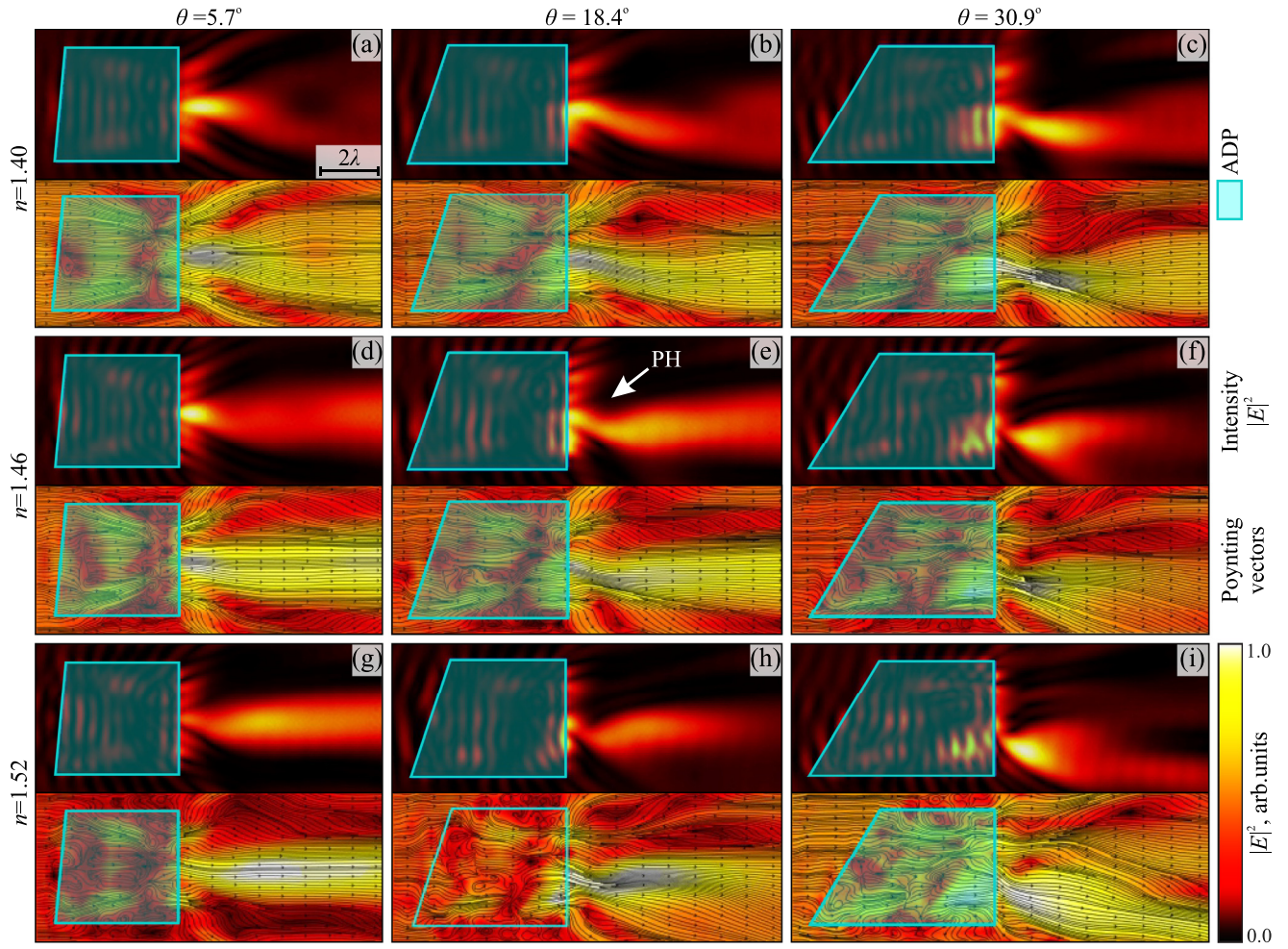


**FIG. 2.** Numerical analysis of the PH formation behind ADP, featuring the rib length of  $L = 4\lambda$  and different refractive indices  $n$  and prism angles  $\theta$ : (a)–(c)  $n = 1.40$  and  $\theta = 5.7^\circ$ ,  $18.4^\circ$ , and  $30.9^\circ$ ; (d)–(f)  $n = 1.46$  and  $\theta = 5.7^\circ$ ,  $18.4^\circ$ , and  $30.9^\circ$ ; (h)–(i)  $n = 1.52$  and  $\theta = 5.7^\circ$ ,  $18.4^\circ$ , and  $30.9^\circ$ . In each panel, the top image represents the EM field intensity  $|E|^2$ , while the bottom image shows time-averaged Poynting vectors. The most pronounced PH is observed in panel (e).

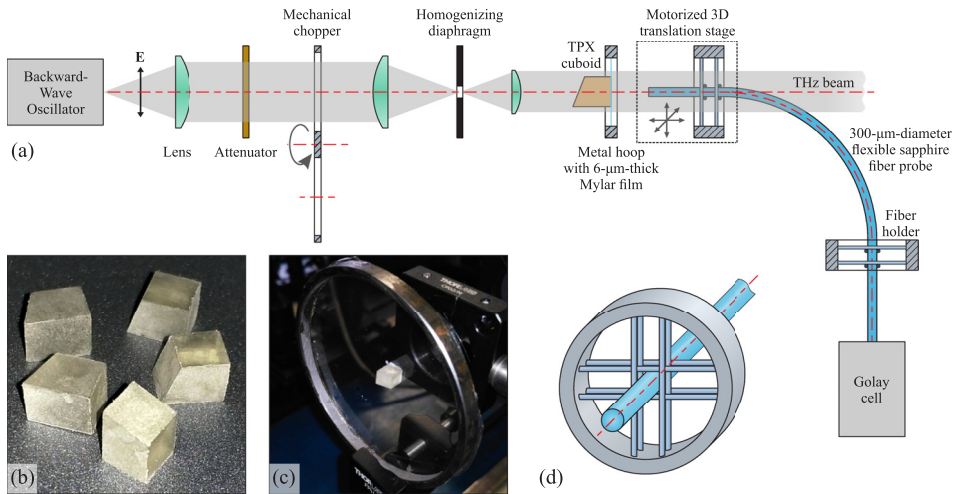


**FIG. 3.** Experimental setup for visualization of the PH relying on principles of the scanning-probe THz imaging and exploiting a flexible 300- $\mu\text{m}$ -diameter sapphire fiber: (a) a scheme of the experimental setup; (b) a photo of the TPX cuboids; (c) a photo of the TPX cuboid glued onto a 6- $\mu\text{m}$ -thick Mylar film mounted on a metal frame; (d) a scheme of the sapphire fiber handling using crossed polymer cords.

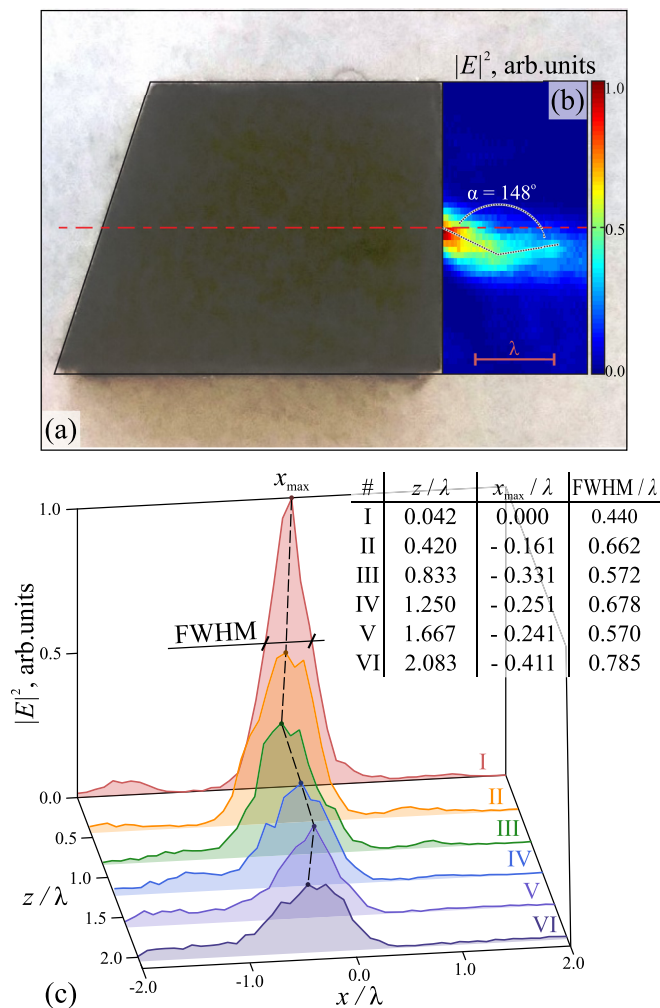


**FIG. 4.** Experimental visualization of a PH with the parameters from Fig. 2(e): (a) a photo of ADP made of TPX; (b) THz field intensity  $|E|^2$ , at the shadow side of a particle illustrating the PH effect; (c) cross-sections of the observed PH. In (c), a table-inset shows parameters of the PH cross-sections.

advantages over common PJ in imaging applications, similar to the beneficial character of the Airy beams over the Gaussian and Bessel ones.<sup>21</sup> Being compared to a symmetric PJ, PH should lead to an increased spatial resolution and an enhanced field of view. However, such an application of PH seems to be a subject of additionally comprehensive study.

The PHs appear even in free space and require no waveguiding structures or external potentials. We believed that the curved trajectory of PH is beneficial to photonics and the related disciplines. It could be used for advanced manipulation of nanoparticles and biological systems, where curved sub-wavelength-scale optical caustics are of interest. Particularly, using numerical methods, it was recently shown that the trajectory of a probe nanoparticle placed in PH is equally curved,<sup>22</sup> and we can make a manipulator to move particles along a curved path around transparent obstacles on a nanoscale.

In contrast to traditional Airy beams, generated using a complicated optical element with a cubic phase or with a spatial light modulator behind the focus of spherical lens, PH can be created using a compact mesoscale dielectric particle-lens. The mesoscale dimensions and simplicity of the PH source enable its integration into lab-on-a-chip platforms.<sup>23</sup> Moreover, Airy beam consists of a main lobe and a family of side beamlets, whose intensity decay exponentially.<sup>2,3</sup> In the case of PH, only main lobe has a curved shape, while the family of curved sidelobes is absent.

Variation of electromagnetic distributions in mesoscale structures is generally known for devices exploiting the multi-mode interference phenomenon.<sup>24</sup> We must emphasize that the experimentally studied particle is not equal to asymmetric couplers or slanted cuboids widely used in multi-mode interference devices;<sup>25-27</sup> the curved sub-wavelength-scale PH is formed in free space behind the dielectric particle but not inside the device “guiding” the light. The generation of PH using known elements of macro-optics appears to be a daunting task.

In conclusion, in this letter, we have experimentally observed the PH phenomenon. It has a general character and should be inherent to acoustic and surface waves, electrons, neutrons, protons, and other beams, interacting with asymmetric mesoscale obstacles. Despite the fact that we considered a simple configuration of the dielectric particle, the observation of the PH phenomenon for different types of asymmetric mesoscale objects, searching for its application in various branches of science and technology, seems to be prospective topics for further research.

An experimental study of K.I.Z. and N.V.C. was supported by Russian Science Foundation, Project No. 17-79-20346. Numerical simulations by L.Y. were supported by Ser Cymru National Research Network (NRNF66) and by Z.W. at the expense of funds received from the H2020 research and innovation program under grant agreement No. 737164. I.V.M. and O.V.M. initiated the study and analysis of experimental and numerical data were in the framework of Tomsk Polytechnic University Competitiveness Enhancement Program.

## REFERENCES

- <sup>1</sup>M. V. Berry and N. L. Balázs, *Am. J. Phys.* **47**, 264 (1979).
- <sup>2</sup>G. A. Siviloglou, J. Broky, A. Dogariu, and D. N. Christodoulides, *Phys. Rev. Lett.* **99**, 213901 (2007).
- <sup>3</sup>G. A. Siviloglou and D. N. Christodoulides, *Opt. Lett.* **32**, 979 (2007).
- <sup>4</sup>I. Kaminer, R. Bekenstein, J. Nemirovsky, and M. Segev, *Phys. Rev. Lett.* **108**, 163901 (2012).
- <sup>5</sup>P. Aleahmad, M.-A. Miri, M. S. Mills, I. Kaminer, M. Segev, and D. N. Christodoulides, *Phys. Rev. Lett.* **109**, 203902 (2012).
- <sup>6</sup>P. Zhang, Y. Hu, T. Li, D. Cannan, X. Yin, R. Morandotti, C. Zhigang, and X. Zhang, *Phys. Rev. Lett.* **109**, 193901 (2012).
- <sup>7</sup>J. F. Healy, *Pliny the Elder on Science and Technology* (Oxford University Press, 1999).
- <sup>8</sup>G. Mie, *Ann. Phys.* **330**, 377 (1908).
- <sup>9</sup>J. Strutt, *Philos. Mag.* **41**, 274 (1871).
- <sup>10</sup>H. J. Münzer, M. Mosbacher, M. Bertsch, J. Zimmermann, P. Leiderer, and J. Boneberg, *J. Microscopy* **202**, 129 (2001).
- <sup>11</sup>Z. Chen, A. Taflove, and V. Backman, *Opt. Express* **12**, 1214 (2004).
- <sup>12</sup>B. S. Luk'yanchuk, R. Paniagua-Dominguez, I. V. Minin, O. V. Minin, and Z. Wang, *Opt. Mater. Express* **7**, 1820 (2017).

- <sup>13</sup>I. V. Minin and O. V. Minin, *Diffractive Optics and Nanophotonics: Resolution below the Diffraction Limit* (Springer, 2016).
- <sup>14</sup>L. Yue, O. V. Minin, Z. Wang, J. N. Monks, A. S. Shalin, and I. V. Minin, *Opt. Lett.* **43**, 771 (2018).
- <sup>15</sup>A. Podzorov and G. Gallot, *Appl. Opt.* **47**, 3254 (2008).
- <sup>16</sup>C.-M. Chiu, H.-W. Chen, Y.-R. Huang, Y.-J. Hwang, W.-J. Lee, H.-Y. Huang, and C.-K. Sun, *Opt. Lett.* **34**, 1084 (2009).
- <sup>17</sup>G. A. Komandin, S. V. Chuchupal, S. P. Lebedev, Y. Goncharov, A. F. Korolev, O. E. Porodinkov, I. E. Spektor, and A. A. Volkov, *IEEE Trans. Terahertz Sci. Technol.* **3**, 440 (2013).
- <sup>18</sup>N. V. Chernomyrdin, A. S. Kucheryavenko, G. S. Kolontaeva, G. M. Katyba, I. N. Dolganova, P. A. Karalkin, D. S. Ponomarev, V. N. Kurlov, I. V. Reshetov, M. Skorobogatiy, V. V. Tuchin, and K. I. Zaytsev, *Appl. Phys. Lett.* **113**, 111102 (2018).
- <sup>19</sup>G. Katyba, K. Zaytsev, I. Dolganova, I. Shikunova, N. Chernomyrdin, S. Yurchenko, G. Komandin, I. Reshetov, V. Nesvizhevsky, and V. Kurlov, *Prog. Cryst. Growth Charact. Mater.* **64**, 133 (2018).
- <sup>20</sup>G. Katyba, K. Zaytsev, N. Chernomyrdin, I. Shikunova, G. Komandin, V. Anzin, S. Lebedev, I. Spektor, V. Karasik, S. Yurchenko, I. Reshetov, V. Kurlov, and M. Skorobogatiy, *Adv. Opt. Mater.* **6**, 1800573 (2018).
- <sup>21</sup>T. Vettenburg, H. I. C. Dalgarno, J. Nylk, C. Coll-Lladó, D. E. K. Ferrier, T. Čizmar, F. J. Gunn-Moore, and K. Dholakia, *Nat. Methods* **11**, 541–544 (2014), available at <https://www.nature.com/articles/nmeth.2922>.
- <sup>22</sup>A. Ang, A. Karabchevsky, I. V. Minin, O. V. Minin, S. V. Sukhov, and A. S. Shalin, *Sci. Rep.* **8**, 2029 (2018).
- <sup>23</sup>C. I. Rogers, K. Qaderi, A. T. Woolley, and G. P. Nordin, *Biomicrofluidics* **9**, 016501 (2015).
- <sup>24</sup>L. Soldano and E. Pennings, *J. Lightwave Technol.* **13**, 615 (1995).
- <sup>25</sup>L. Han, S. Liang, H. Zhu, L. Qiao, J. Xu, and W. Wang, *Opt. Lett.* **40**, 518 (2015).
- <sup>26</sup>X. Sun, J. Aitchison, and M. Mojahedi, *Opt. Express* **25**, 8296 (2017).
- <sup>27</sup>P. Wang, H. Zhao, X. Wang, G. Farrell, and G. Brambilla, *Sensors* **18**, 858 (2018).